HOKKAIDO UNIVERSITY

Title	Synergistic Effect of the Oleic Acid and Oleylamine Mixed-Liquid Matrix on Particle Size and Stability of Sputtered Metal Nanoparticles
Author(s)	Mai Thanh Nguyen; Wongrujipairoj, Krittaporn; Tsukamoto, Hiroki; Kheawhom, Soorathep; Mei, Shuang; Aupama, Vipada; Yonezawa, Tetsu
Citation	sustainable chemistry & engineering, 8(49), 18167-18176 https://doi.org/10.1021/acssuschemeng.0c06549
Issue Date	2020-12-14
Doc URL	http://hdl.handle.net/2115/83513
Rights	This document is the Accepted Manuscript version of a Published Work that appeared in final form in Sustainable chemistry & engineering, copyright c American Chemical Society after peer review and technical editing by the publisher. To access the final edited and published work see https://pubs.acs.org/doi/10.1021/acssuschemeng.0c06549.
Type	article (author version)
Additional Information	There are other files related to this item in HUSCAP. Check the above URL.
File Information	(1) Revised manuscript.pdf

Instructions for use

Hokkaido University Collection of Scholarly and Academic Papers : HUSCAP

Synergistic Effect of Oleic Acid and Oleylamine Mixed Liquid Matrix on Particle Size and Stability of Sputtered Metal Nanoparticles

Mai Thanh Nguyen,[1,*] Krittaporn Wongrujipairoj,[1,2] Hiroki Tsukamoto[1], Soorathep Kheawhom,[2] Shuang Mei,[1] Vipada Aupama,[1,2] Tetsu Yonezawa[1,3,*]

[1]Division of Materials Science and Engineering, Faculty of Engineering, Hokkaido University, Kita 13 Nishi 8, Kita-ku, Sapporo, 060-8628, Japan

[2]Department of Chemical Engineering, Faculty of Engineering, Chulalongkorn University, Bangkok 10330, Thailand

[3]Institute of Business-Regional Collaborations, Hokkaido University, Kita 21 Nishi 11, Kita-ku, Sapporo, 001-0021, Japan

*Email: mai_nt@eng.hokudai.ac.jp, tetsu@eng.hokudai.ac.jp

Abstract

This research investigates the impact of mixing oleylamine and oleic acid as the liquid matrix for sputtering of metal nanoparticles and the mixed liquid composition on the particle size, uniformity, and their colloidal and oxidation stability. The case study was conducted for Au and Cu which are noble and non-noble metal, respectively. The results reveal that the mixed liquids are more effective in producing smaller and more uniform metal nanoparticles. Smallest Au nanoparticles with highly colloidal stability over a year were obtained with equal volume of OA and OAm. OA/OAm 1/1 (v/v) also exhibited the best protection effect from oxidation for Cu nanoparticles. The results can be attributed to the improved viscosity and synergistic protecting capability of the mixed liquids compared with the single component liquids.

Keywords: Matrix Sputtering, Oleic acid, Oleylamine, Metal Nanoparticles, Gold, Copper, Colloidal Stability, Oxidation Suppression

Introduction

Sputtering onto liquid has been emerging as a green and new technique for producing nanoparticles dispersed in liquid from the bulk metal foil/plates.[1-12] The liquid matrix serves as a tool to manipulate the formation and growth, characteristics, and properties of nanoparticles.[13-26] Because sputtering occurs under vacuum conditions, some liquids with low vapor pressures have been used as the matrix, for example, liquid polymer/monomer (silicone oil,[1] polyethyleneglycol (PEG),[6,22,23] glycerol,[9] pentaerythritol ethoxylate (PEEL),[14] pentaerythritol tetrakis(3-mercaptopropionate) (PEMP)[15]), ionic liquid,[2-3,8,10,16-21,24] vegetable oil,[5,7] and molten salt.[4] The method allows for obtaining not only metal, [1,5-11] oxide,[14,21] and alloy[3,12-20,22-24] nanoparticles but also small nanoclusters.[4,15,25,26]

The studies in this field reveal important roles of the liquid matrix in the growth behavior, size control, and colloidal stability of the sputtered nanoparticles.[1-6,13-19,24-40] Evaluating the impact of the physicochemical properties of the liquids on the particle size helped understand the particle formation.[6,18,19,27-38] For example, when Au was sputtered onto ionic liquids, the particle nucleation could occur on the liquid surface and growth could occur on the liquid surface and/or in the bulk liquid.[27-31] The surface tension and composition affect initial nucleation and staying of particles on the liquid surface[27,29,30] whereas the temperature,[27,31] thereby viscosity,[27] and composition[28,29] of the liquid control the growth, particle size, and aggregation of the particles in the bulk liquid during and after sputtering. Here, a higher temperature, thereby a lower viscosity, increases the collision of clusters in an ionic liquid, causing particle growth and aggregation.[27] Composition of the ionic liquid influences the

interaction of liquid with particle and viscosity of the liquid regulates particle collision. This consequently mediates the particle nucleation, growth, and stability.[27,29] Different from ionic liquids, when a liquid mercaptan, *i.e.*, PEMP, or PEG or glycerol was used as the matrix for sputtering of Ag nanoparticles, an increase in viscosity, however, led to a larger particle size and/or a thin film on the liquid surface.[33,35] This suggests the nucleation and growth of particles occurred on the surface of the viscous liquid. On the other hand, lowering the viscosity allowed for the nanoparticles falling into the PEMP; the thiol group of the PEMP matrix tightly bound to the surface of nanoparticles and stabilized them, thus, no further growth as observed in ionic liquids.[35] Addition of a thiol capping agent[36-38] to the based liquid, such as PEG, has been also efficient to obtain small size, fluorescent metal nanoclusters by sputtering onto liquid. In contrast, sputtering of Au, Ag, and/or their alloys onto pure liquid PEG, which weakly binds to the particles, often resulted in big agglomerates, aggregations, and precipitates after a week to several months of storage.[6,37,39] Thus, choosing a liquid matrix for sputtering is important for achieving desired particle formation and size and good dispersion stability.

Aside from regulating particle size and colloidal stability via binding and mediating particle growth, the liquid matrix has an impact on the chemical stability of the formed nanoparticles as reported for Cu.[41-43] Our previous researches show that sputtering onto liquid polymers such as PEEL and PEG (M.W. = 600) produced plasmonic Cu nanoparticles of 2-6 nm.[42,43] However, they were quickly oxidized with an observation of complete fading of the localized surface plasmon resonance after a week.[42,43] On the other hand, adding thiol molecules, *e.g.*, mercaptoundercanoic acid (MUA), to PEG helped produce Cu nanoclusters with negligible change for a month.[36] Upon changing the liquid substrate from PEG containing MUA to PEMP with a rich thiol moiety, *i.e.*, four thiol group in a molecule, Cu nanoclusters were converted to copper sulfides over time.[15] Thus, aside from thiol compounds, liquids with other functional groups should be investigated for stabilizing and protecting Cu nanoparticles.

In the present study, we propose to use oleic acid (OA) paired with oleylamine (OAm) as the liquid matrices for sputtering of metal nanoparticles with controlled particle sizes and stability. They are commonly used ligands and solvents in colloidal synthesis of nanoparticles. Each liquid can act as the capping agent for metal nanoparticles via binding its functional group with the particle surface and as the liquid matrix to disperse the formed nanoparticles. In combination, they can create acid-base complex and hydrogen bonding[43] to modify not only the composition and viscosity of the mixture but also the functionality of the mixtures for stabilizing metal nanoparticles. With using neither high temperature nor additional reducing agents, we can expect to obtain small metal nanoparticles by sputtering onto OA/OAm. Further, varying the ratio of OA and OAm, we could investigate the influence of mixing OA and OAm to the particle size and the stability of the dispersion during storage. We found that among OA, OAm, and OA/OAm liquids, equal volume OA/OAm is the most effective for producing Au nanoparticles with small size, high uniformity, and good colloidal stability over a year. This liquid also allowed for making stable concentrated dispersion of Au nanoparticles. Besides, compared with the single component liquid, the mixed liquids showed an improved oxidation suppression for Cu nanoparticles. The result can be attributed to a higher viscosity and synergistic protection capability of the mixed liquids over the single component ones.

Experimental

Materials. OA and OAm were purchased from Sigma Aldrich. Au 99.99 % and Cu 99.5 % pure targets (ϕ50 mm, 3 mm thickness) were purchased from Nilaco, Japan and used as received. Ethanol, methanol, and hexane were used as received.

Sputtering of metal nanoparticles. OA and OAm were distilled under reduced pressure and then vacuum dried at 120 °C. After that a solution of OA and OAm with a total volume of 10

cm^3 was prepared by mixing OA and OAm at various volume ratios: 1/0, 3/1, 1/1, and 1/3 (v/v) and used as the liquid matrix for magnetron sputtering. The volume ratio of OA and OAm was used to name the samples, for example, Au OA/OAm 1/3 means Au nanoparticles synthesized using OA and OAm with 1/3 (v/v). Noted that the volume ratio is similar to the molar ratio of OA and OAm. OA and OAm were added to a petri dish (ϕ 63 mm) and placed in the sputtering chamber. The distance between the surface of the liquid and metal target (Au or Cu) was set 6 cm. The sputtering chamber was vacuumed and purged with Ar gas multiple times (≥10 times). The pressure was set 2 Pa with Ar as the processing gas, then sputtering was initiated. The target was cleaned via 10 min sputtering to remove surface layers and during this period a shutter was used to cover the liquid matrix. Then, the liquid was exposed to collect metal nanoparticles. The sputtering was performed at a current of 20 mA for 30 min for Au and 30 mA for 1 h for Cu. During sputtering, the liquid was kept at 25 °C and stirred at 80 rpm. The produced samples were analyzed using UV-Vis and TEM immediately after sputtering and after various times of storage (0.5 h to 540 days) in air in a 12 mL glass container. The scheme of the sputtering set-up has been reported elsewhere.[14,15,34,36,43] We noticed that using only OAm as the liquid in sputtering did not allow for a stable plasma, possibly because OAm continuously evaporates in the vacuum chamber.

Copper(II) oleate, of which UV-Vis spectrum was used for comparison with that of the sputtered dispersions of Cu during storage, was prepared by referring to the published method for the synthesis of iron oleate.[45] Instead of iron salt,[45] in the present study $CuCl_2$ was used.

Characterization. After sputtering, metal nanoparticles in OA/OAm were analyzed using a Shimadzu-1800 UV-Vis spectrophotometer and a quartz cell with 1 mm and 10 mm optical path for Au and Cu samples, respectively. UV-Vis spectra for Au samples were collected from 0 h to 540 days after sputtering. UV-Vis spectra for Cu samples were collected from 0.5 h to a week after sputtering. Samples were kept in glass bottles with caps under air. The morphology

of the metal nanoparticles was observed using a transmission electron microscopy (TEM, JEOL JEM 2010 and FX2000, at 200 kV). TEM samples were prepared by dipping a TEM grid to the dispersion and washed with hexane. The size distribution was plotted after measuring the size of 200 or more particles in TEM images. The structure of the nanoparticles was examined using X-ray diffraction (XRD, Rigaku Miniflex II X-ray diffractometer, Cu Kα, 1.5418 Å, radiation). Fourier-transform infrared (FT-IR) spectra of pure OA, OAm, and Au nanoparticles capped with OA/OAm were collected using a Jasco FT/IR-4600 equipped with ATR. The nanoparticles used for XRD and FT-IR analysis were purified using hexane and excessive acetone. Precipitates of particles were obtained after keeping over night or after centrifugation. The process was repeated several times. In most cases, nanoparticles can be redispersed in hexane. Viscosities of OA/OAm liquids were measured using a Brookfield HBDV-I Prime viscometer at 25 °C with a rotation speed of spindle from 4 to 100 rpm (shear rate from 30 to 750 s^{-1}).

Results and Discussion

Au nanoparticles sputtered onto OA/OAm liquid matrix with various volume ratios

TEM images and size distribution of Au nanoparticles obtained after sputtering are shown in **Figure 1**. Using only OA resulted in Au nanoparticles of 5.0 ± 1.5 nm (Figures 1a and 1e). By adding OAm to OA, the particle size decreased to 3.3 ± 0.8 nm (Au OA/OAm 3/1, Figures 1b and 1f) and 2.4 ± 0.4 nm (Au OA/OAm 1/1, Figures 1c and 1g). However, a further increase of OAm (OA/OAm 1/3) did not help reduce the particle size any further. This resulted in the formation of Au with both small (3.4 ± 0.6 nm, Figures 1d and 1h) and big sizes (>10 nm, inset of Figure 1d). The particle size distribution (Figures 1e - 1h) reveals that the most uniform Au nanoparticles were obtained with OA/OAm 1/1. Au OA/OAm 1/0 contained some agglomerations and big particles of > 10 nm which was dominant in Au OA/OAm 1/3. UV-

Vis spectra of these samples are consistent with the TEM observation. Typical localized surface plasmon resonance (LSPR) of Au at 515 nm was observed in the UV-Vis spectra of Au OA/OAm 1/0, 3/1, and 1/3. The broad absorption at long wavelength (~700 nm) for Au OA/OAm 1/0 agrees with TEM result on the presence of some Au agglomeration, which reflects in the violet color of the dispersion (Figure 1j). The low intensity of Au OA/OAm 1/3 is caused by the fact that big size nanopartiles as the major fraction of the sample forming Au film (Figure 1k) precipitated and assembled in the glass container (**Figure S1**) while small Au particles remained dispersed in liquid OA/OAm for UV-Vis measurement. The LSPR peak is not obvious for Au OA/OAm 1/1, which is consistent with small particle size, 2.4 ± 0.4 nm, as observed in the TEM image (Figures 1c and 1g). Thus, these primary results indicate that mixing OA with OAm allows for tailoring the particle size and uniformity.

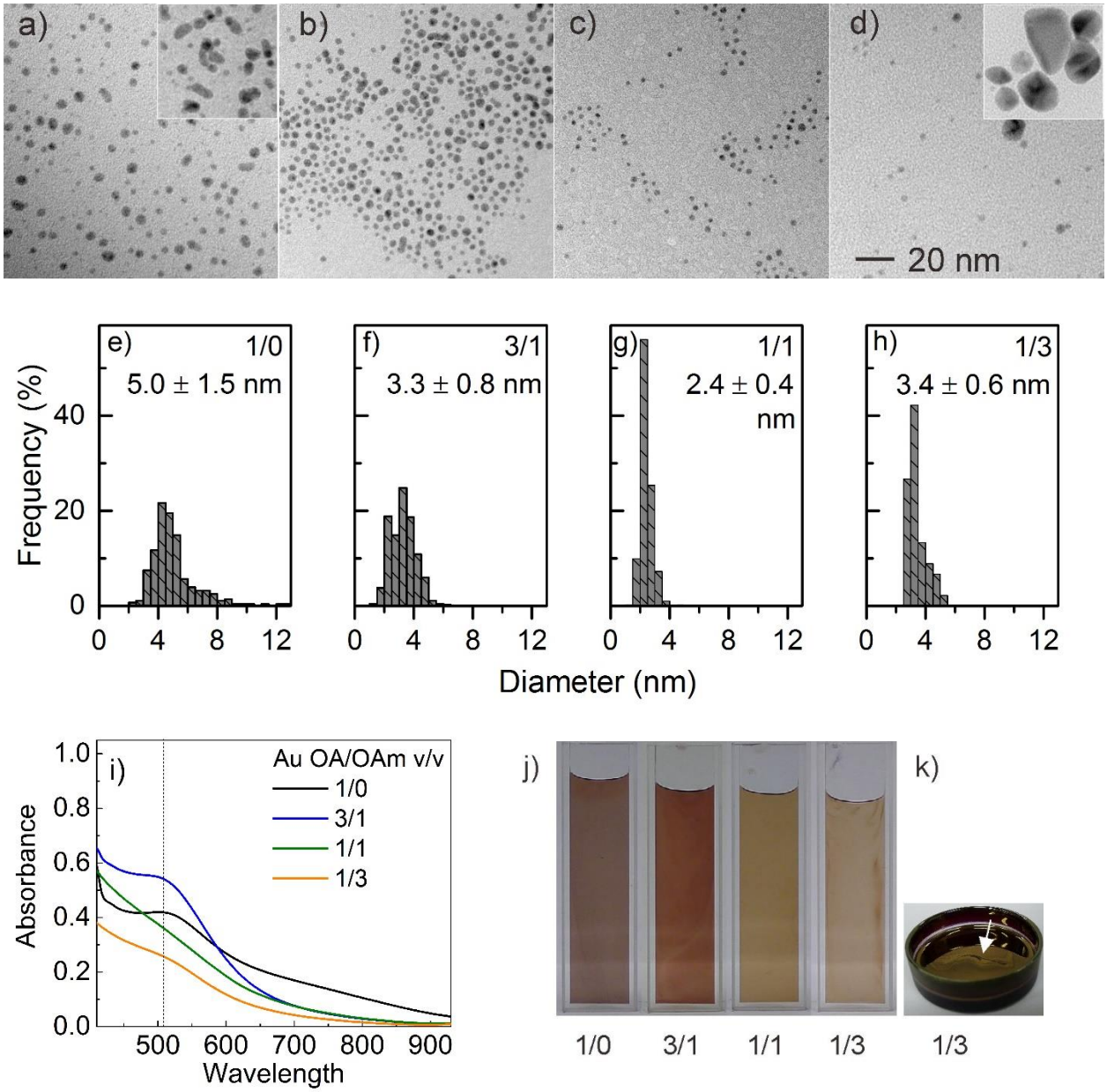

Figure 1. (a-d) TEM images and (e-h) size distributions of as-synthesized Au nanoparticles by sputtering onto liquid OA/OAm of (a, e) 1/0, (b, h) 3/1, (c, g) 1/1, and (d, h) 1/3 (v/v). The inset of (d) shows Au particles of more than 10 nm (so-called big nanoparticles) as the minor in the liquid dispersion of Au OA/OAm 1/3 sample. (i) UV-Vis spectra of as-synthesized Au nanoparticles prepared using various OA/OAm volume ratios wherein the dashed line at 515 nm is added for the visual guide of the LSPR peak position of Au nanoparticles. (j) Photos of Au OA/OAm dispersions in quartz cuvettes with 1 mm optical path used for taking the UV-Vis spectra. (k) Au film formed on surface of OA/OAm 1/3 with the arrow pointing to the film.

Particle growth and colloidal stability of Au nanoparticles during storage

The change of the particle size and the stability of the sputtered Au nanoparticles dispersed in OA/OAm over times, 0-540 days of storage, were studied. The results of the particle sizes measured from TEM images are summarized in **Table 1** and plotted in **Figure 2**. TEM images of the samples after 100 days of storage are shown in **Figure 3** whereas the TEM images of samples stored for other periods of time with the corresponding size distribution are shown in **Figures S2-S7**.

Figure 2a reveals that among the four samples and for any storage time, OA/OAm 1/1 stabilized Au nanoparticles always possess the smallest size and the best uniformity. When the storage time increased, the particle size of this sample increased from 2.4 ± 0.4 nm (as-synthesized) to 2.5 ± 0.6 nm (14 days), 3.2 ± 0.5 nm (52 days), and 3.6 ± 0.4 nm (100 days, Figure 3). After that, the mean size did not increase any further while the size distribution was slightly broader, that is 3.6 ± 0.9 nm after 540 days of storage.

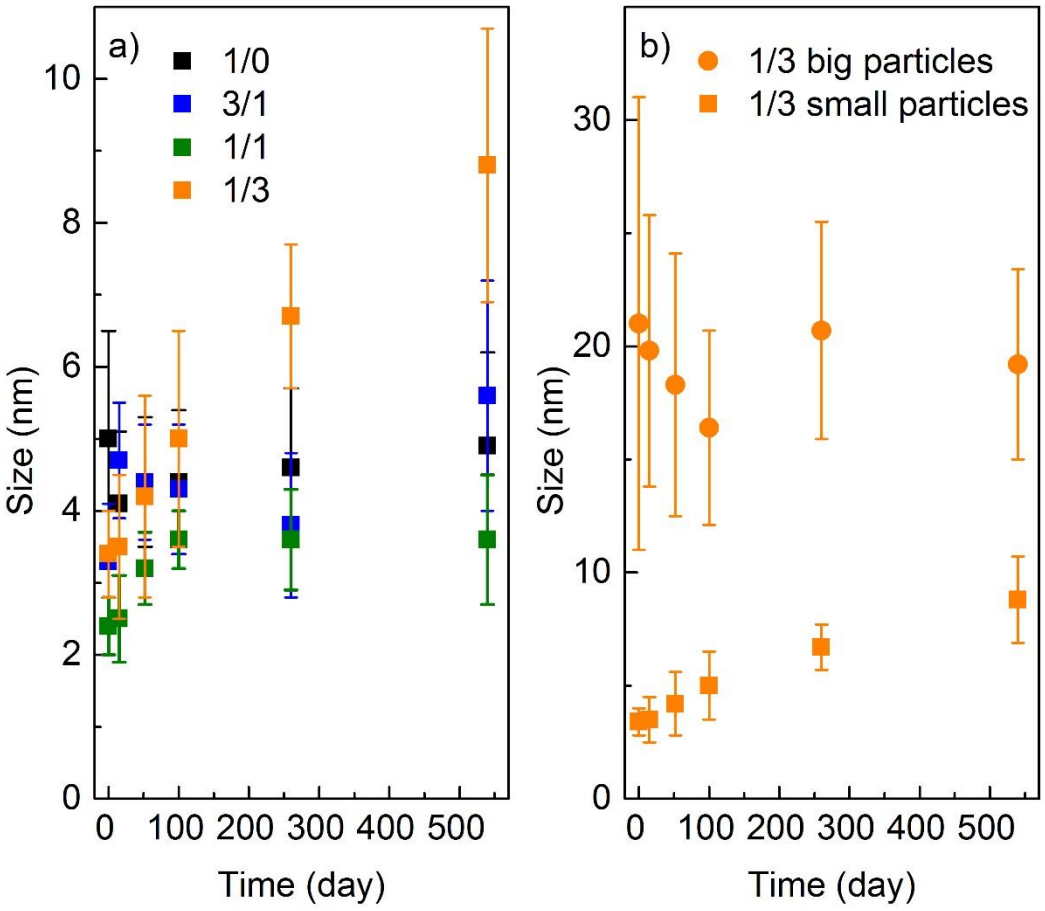

Figure 2. (a) Particle size of Au nanoparticles dispersed in OA/OAm liquids for various storage times. (b) Particle size of big Au OA/OAm 1/3 at the bottom and/or on the wall of the storage container. The bars represent the standard deviation of the particle size.

Table 1. Particle size of Au nanoparticles sputtered onto OA/OAm liquids during storage

Particle size during storage (nm) [a]	**Au OA/OAm (v/v)**				
	1/0	**3/1**	**1/1**	**1/3 (small)**	**1/3 (big)**
0 day	5.0 ± 1.5	3.3 ± 0.8	2.4 ± 0.4	3.4 ± 0.6[b]	11.0~31.0[b]
15 days	4.1 ± 1.0	4.7 ± 0.8	2.5 ± 0.6	3.5 ± 1.0	19.8 ± 6.0
52 days	4.4 ± 0.9	4.4 ± 0.8	3.2 ± 0.5	4.2 ± 1.4	18.3 ± 5.8
71 days	4.1 ± 1.0	4.0 ± 0.8	3.5 ± 0.3	4.3 ± 1.2	15.1 ± 2.8
100 days	4.4 ± 1.0	4.3 ± 0.9	3.6 ± 0.4	5.0 ± 1.5	
	4.7 ± 0.9[c]	5.1 ± 0.9[c]			16.4 ± 4.3 [c]
260 days	4.6 ± 1.1	3.8 ± 1.0	3.6 ± 0.7	6.7 ± 1.0[c]	20.7 ± 4.8[c]
540 days	4.9 ± 1.3	5.6 ± 1.6	3.6 ± 0.9	8.8 ± 1.9	19.2 ± 4.2 (solid)
540 days, XRD, liquid part[d]	4.2	3.3	3.5	6.2	
540 days, XRD, bottom part[d]	5.4	5.3	3.7		10.5 8.9[e]

[a]The particle size measured from TEM images of 300-600 particles. [b]The number of nanoparticles for measuring particles size is less than 100. [c]The size of nanoparticles obtained at the bottom of the storage glass container which contain precipitate or agglomerates observed in OA/OAm 1/0, 3/1 and 1/3 but not in 1/1 (v/v). [d]The grain size of nanoparticles estimated from the line broadening of the main XRD peak using Scherrer equation. Big nanoparticles are the major population in TEM images of Au OA/OAm 1/3 after 15 days. [e]Grain size of big nanoparticles which were redispersed well in hexane.

In general, the increase of particle size over time was also observed for samples Au OA/OAm 1/0 and 1/3 but at larger amounts of increase compared with that of sample Au OA/OAm 1/1. The mean particle size of Au OA/OAm 1/0 sample slightly increased after 100 days (100 days: 4.4 ± 1.0 nm; 540 days: 4.9 ± 1.3 nm) whereas that of small nanoparticles in sample Au OA/OAm 1/3 kept increasing almost linearly with time from the 0 to 540 days of storage (0 day: 3.4 ± 0.6 nm, 100 days: 5.0 ± 1.5 nm; 540 days: 8.8 ± 1.9 nm). Interestingly, during the storage from day 0 to 100, the particle size of big nanoparticles in sample Au OA/OAm 1/3 decreased with time (**Figure 2b**). With increasing storage time, agglomeration of big Au particles (>10 nm) becomes more dominant. Their agglomerations assembled and gathered on the surface of the glass bottle used for containing the sample (**Figure 4g**). The

phenomena suggest that the size-focusing occurred in the sample during storage. The results of particle size for sample Au OA/OAm 1/0 shows that a decrease occurred first (15 days of storage) and followed by a gradually increase in particle size. The decrease of particle size in the initial storage period can be caused by the dissolution of the big particles and their agglomerations in OA which is attributed to the repulsive force of Au coated OA as reported by Fujita *et al*.[40] The disappearance of the optical absorption in long wavelength (**Figure S8**) compared with that of the as-synthesized sample (Figure 1i) is in good aggreement with the TEM result of the size focusing after 15 days of storage. In contrast, particle size of Au OA/OAm 3/1 first increased (4.7 ± 0.8 nm, 15 days), then slightly decreased with storage time up to 260 days (100 days: 4.3 ± 0.9 nm; 260 days: 3.8 ± 1.0 nm), and finally reached 5.6 ± 1.6 nm (540 days). UV-Vis spectra of this sample during storage show similar phenomenon as observed for Au OA/OAm 1/0, which indicates the size focusing and growth of Au.

Regarding the colloidal stability of the dispersion, it is noticeable that Au OA/OAm 1/1 is the only sample which did not have any precipitation during storage (0-540 days). The precipitation was not observed clearly in other OA riched samples, *e.g.*, Au OA/OAm 1/0 and 3/1, but there were agglomerations or highly concentrated Au nanoparticles gathering at the bottom of the samples for 100 days of storage or longer (**Figures S8e and S9**). Such agglomerations comprised of Au nanoparticles with sizes, that is 4.7 ± 0.9 nm (Au OA/OAm 1/0, Figures 4a, 4d, and 4h) and 5.1 ± 0.9 nm (Au OA/OAm 3/1, Figures 4b, 4e, and 4i), slightly bigger than the ones in the bulk liquid. In contrast, Au OA/OAm 1/3 contained precipitates at the bottom and assembly of big Au nanoparticles with a mean size of 16.4 ± 4.3 nm (Figures 4c, 4f, and 4j) on the wall of the glass bottle (Figure 4g). The longer the storage time, the more nanoparticles join the assembly and the more dilute the dispersion of the small Au nanoparticles in the top liquid.

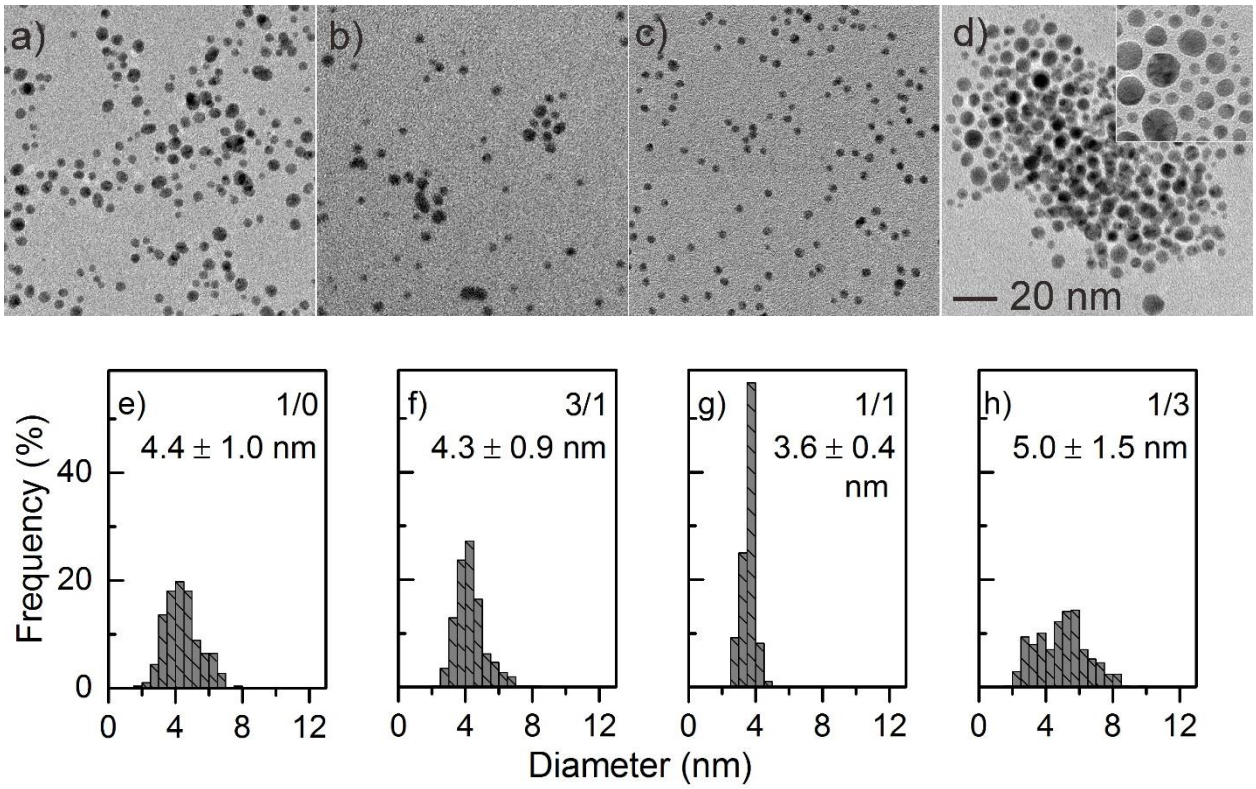

Figure 3. (a-d) TEM images and (e-h) size distribution of Au nanoparticles sputtered onto OA/OAm liquids of (a) 1/0, (b) 3/1, (c) 1/1, and (d) 1/3 (v/v) after stored for 100 days. The inset of (d) shows particles near the bottom of the container.

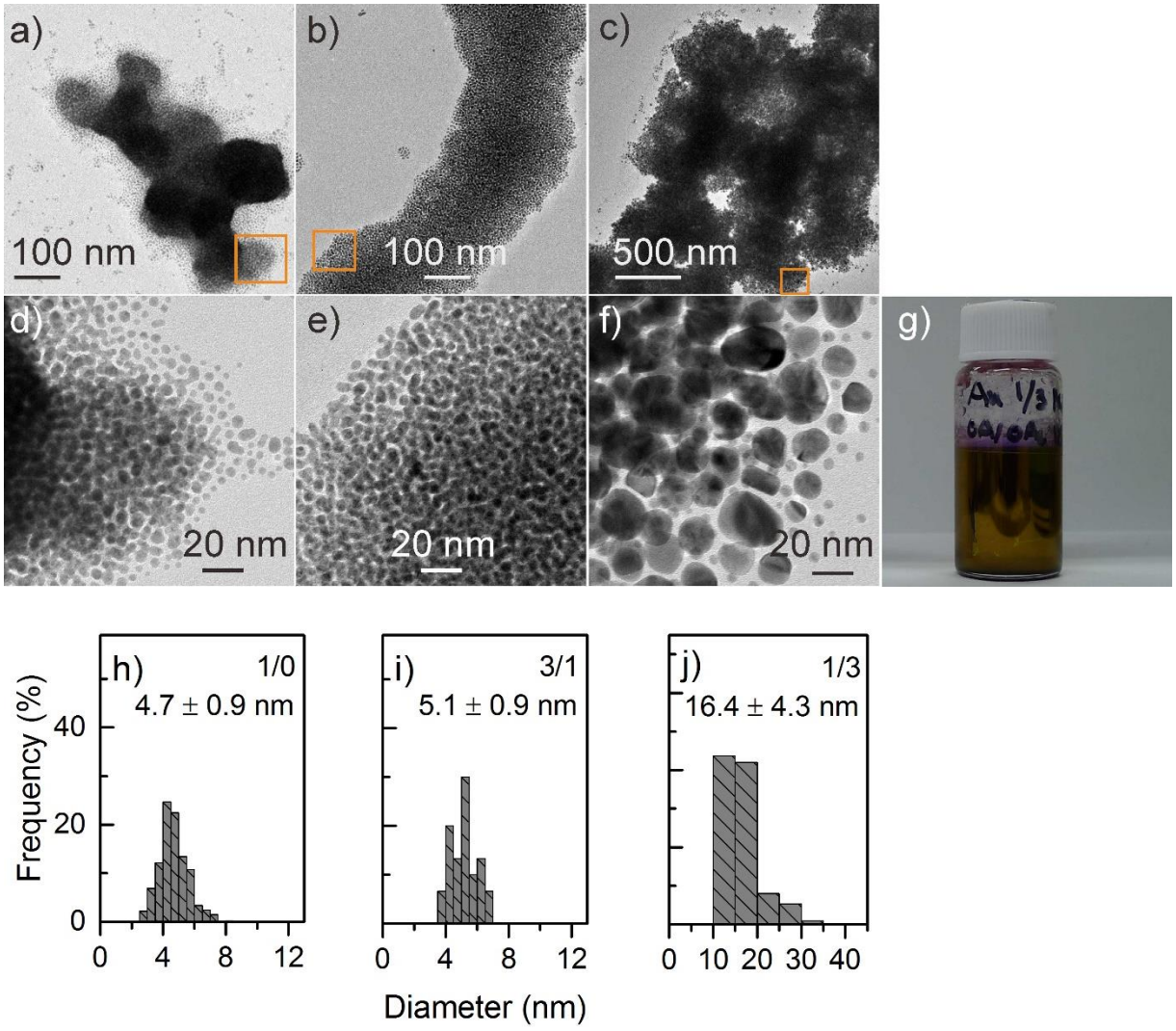

Figure 4. (a-f) TEM images and (h-i) size distribution of Au nanoparticles at the bottom of OA/OAm liquids of (a, d, h) 1/0, (b, e, i) 3/1, and (c, f, j) 1/3 (v/v) after stored for 100 days. (d-f) are zoom-in images of the particles in orange squares in (a-c). (g) Photograph of Au OA/OAm 1/3 in the container for storage.

The grain sizes of Au nanoparticles estimated from XRD line broadening (**Figure 5**) using Scherrer equation are consitent with the results obtained from TEM observation (Figure S7) for samples stored for 540 days. Aggromerates or precipitates at the bottoms of Au OA/OAm 1/0, 3/1 and 1/3 have bigger particle size and grain size compared with Au nanoparticles dispersed in the upper liquid (Table 1). It also suggests that the small Au nanoparticles are

likely single crystal while the big Au nanoparticles (*i.e.*, in Au OA/OAm 1/3) are polycrystal, which is consistent with the HR-TEM results (**Figure S10**). Judging from the change of particle size and the colloidal stability, it is clear that the equal volume OA/OAm liquid matrix provides the best colloidal stability for Au nanoparticles.

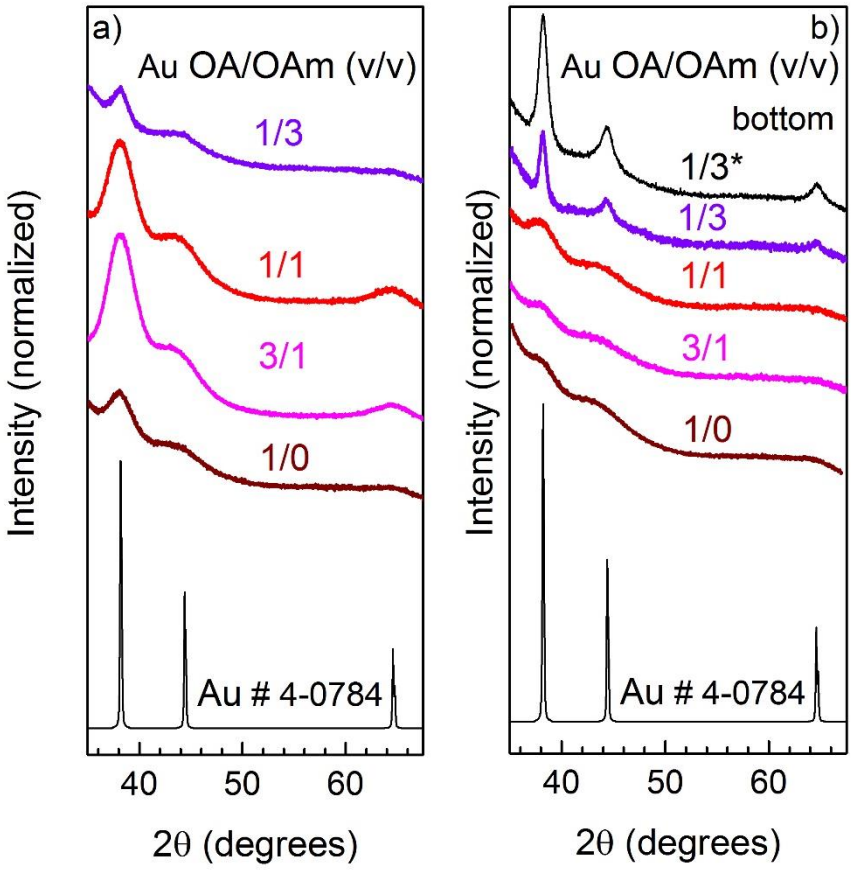

Figure 5. XRD patterns of Au OA/OAm 1/0, 3/1, 1/1, and 1/3 after 540 days stored in OA/OAm from (a) particles in the bulk liquid and (b) the bottom part of the dispersion containing some agglomerates or solids. The black pattern marked with star is for Au OA/OAm 1/3 of the bottom part which could be well re-dispersed in hexane.

Discussion: Impact of OA/OAm volume ratios on the particle size and colloidal stability

From the observation of the particle size, the size increase during storage, and the colloidal stability, it is obvious that OA/OAm 1/1 liquid is efficient for obtaining small and uniform Au nanoparticles. Using pure OA and OA-rich mixed liquids, that is, OA/OAm 1/0 and 3/1, results in Au nanoparticles (<10 nm) with slightly bigger size and less uniformity. In contrast, big Au nanoparticles of about 20 nm, which precipitated and assembled over time of storage, were achieved with OAm-rich liquid, that is, OA/OAm 1/3. The impact of the liquid on the size of nanoparticles produced by sputtering onto liquid and particle growth can be caused by several factors such as the viscosity of the liquid and their capping capability which play important roles in particle growth. De Luna et al. have reported that a viscous liquid which does not bind strongly with particle surface can lead to the formation of a thin metal film on the liquid surface.[33] In contrast, a liquid with suitable viscosity can allow the sputtered nanoparticles to fall into it and also the liquid can stabilize the nanoparticles from collision and growth.[27,28,33,35] The chemical properties of the liquid are important in stabilizing the formed nanoparticles. Torimoto et al. reported the tunable size of Au nanoparticles from 1.9 to 5.5 nm by varying the ionic liquids as the matrix for sputtering.[2] Using liquid polyethylene glycol, Au nanoparticles were also obtained.[6] However, owing to the weak capping of PEG to Au nanoparticles, the particles have bigger size (3-5 nm)[6,39] and less colloidal stability (precipitate and agglomerations after few weeks of storage).[6,39] The addition of thiol ligands, which strongly bind to the surface Au as well as other metals, to PEG significantly reduce the particle size and improve the colloidal stability of metal nanoparticles and clusters.[26,36-38] Thus, we need to consider both the viscosity and the capping power of the liquid when discussing its impact on size control, particle growth, and colloidal stability. In the present study, OA and OAm are viscous liquids with carboxylic and amine groups, respectively. The functional group of OA

and OAm can bind to the surface of the nanoparticles and therefore help stabilize Au nanoparticles.

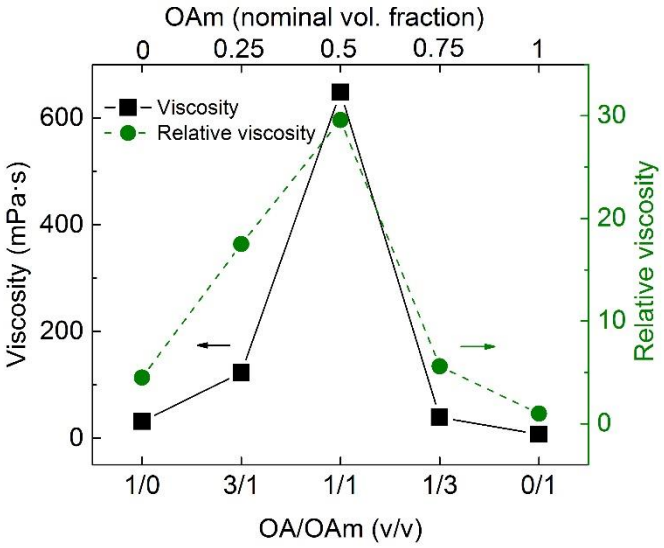

Figure 6. Viscosity of OA/OAm liquid (black filled squares) with various volume ratios of OA and OAm. Relative viscosity of a liquid (green filled circle) is estimated by dividing its viscosity by the viscosity of OAm. All liquids exhibit Newtonian behavior in the measurement range (shear rate from 30 to 750 s^{-1}) at 25 °C. Dashed and solid lines connecting the data points are for visual guide.

Figure 6 shows the viscosity of OA, OAm, and the mixed liquids. The viscosity substantially increases by mixing OA and OAm with the peak belonging to OA/OAm 1/1. OAm has the lowest viscosity followed by OA whereas OA/OAm 1/1 has viscosity about 30 times of that of OAm. This result explains for the small size and good stability of Au OA/OAm 1/1 sample compared with others.

However, the viscosity itself could not explain everything. Particularly, viscosity of OA/OAm 1/0 liquid is close to that of OA/OAm 1/3 and almost half of that of OA/OAm 3/1.

However, the Au nanoparticles produced in the OA/OAm 1/0 has the size similar to Au OA/OAm 3/1 while much smaller than Au OA/OAm 1/3. This is to say, the particle size is not solely controlled by the liquid viscosity. Therefore, the interaction of OA and OAm and their combination effect for stabilizing the nanoparticles should be taken into account. OA and OAm can interact with each other and the deprotonation of carboxylic group in OA can occur, resulting in the formation of carboxylate anion and amine cation. The electrostatic interaction of the formed ions is possibly stronger than the weak Van der Waals one in OA or OAm itself. Thus, mixing OA and OAm can improve the viscosity. Further, the carboxylate anion and/or amine cation bind stronger to the surface of nanoparticles for more effectively stabilizing nanoparticles, leading to formation of nanoparticles with small sizes. Especially, carboxylate can make bidentate binding to metal particles which is believed stronger than binding via monodentate or amine group. Therefore, OA/OAm 1/1 resulted in smallest and most stable Au nanoparticles. Even without OAm, OA can deprotonate to some extent, forming carboxylate anion which has good binding with particle surface. However, this process is not that much in pure OAm. Thus, the stronger binding of OA compared with OAm to the particle surface can be expected. The deprotonation of OA becomes more easily and occurs to a larger fraction of the OA molecules when OAm is added. This can explain for the big difference in the particle size obtained using OAm-rich liquid, that is OA/OAm 1/3, and OA-rich liquids, that is, OA/OAm 1/0 and 3/1 even though their viscosities are not substantially different.

After purification, the nanoparticles can be easily re-dispersed in hexane, indicating that the carboxylic and amine functional group bind to the particle surface and the alkyl tails heading towards to hydrophobic solvent. To get more in depth of the OA/OAm stabilized Au nanoparticles, the FT-IR patterns of the purified nanoparticle samples and the pure liquids at various volume ratios were collected (**Figure 7**). Figure 7a shows the symmetric and as-symmetric stretching of (-CH_2-) at 2853 and 2925 cm^{-1}, respectively, and bending of C-H

bonding in C=CH and of -CH_3 group at 3006 and 1465 cm^{-1}, respectively, for all Au samples, which is also identical to pure OA, OAm, and mixed OA/OAm liquids (Figure 7b). These signals come from the unsaturated alkyl tails of OA and OAm, indicating the presence of the capping ligand on the particle surface. The stretching of C=O at 1712 cm^{-1} (in –COO group) was observed for Au OA/OAm 1/0, 3/1, and 1/1 but not visible in Au OA/OAm 1/3. Similar phenomenon was observed in liquid OA/OAm 1/3 without Au. The decrease of FT-IR peak from C=O in the Au OA/OAm is consistent with what was observed in the mixed liquid. This indicates the formation of carboxylate anion (R-COO^-) and amine cation (R-NH_3^+) in the mixed liquids, which makes the free C=O stretching disappear.

The peaks at 1542 (Au OA/OAm 1/0 and 3/1), 1559 (Au OA/OAm 1/1), and 1569 cm^{-1} (Au OA/OAm 1/3) belong to the bidentate of carboxylic group (-COO^-) with Au surface.[46,47] The peak from the bindentate of carboxylic group is significant compared with the weak bending mode at 1581 cm^{-1} of –NH_2 in OAm.[46] With an increase in OAm used in the liquid matrix, the peak from bidentate -COO–Au shifts to a longer frequency. Similar phenomenon was observed for the mixed liquids themselves wherein no carboxylate peak associated with pure OA. The significant signal from carboxylic anion and substantial decrease of free C=O in the mixed liquids compared with pure OA indicates that adding OAm to OA helped generate carboxylate and/or OA-OAm complex for binding and stabilizing the metal nanoparticles. The peak marked by black dashed line at 1654 cm^{-1} appeared in all mixed liquids and Au OA/OAm 1/0, 3/1, 1/1, and 1/3 samples can be assigned for as-symmetric mode of carboxylate group[46] and/or –C=O stretching in amide compounds.[48] It is not likely that this peak belongs to –C=C bending mode which was observed very weak and at higher wavenumbers in pure OA and OAm.[49] Because the peak associated with carboxylate and/or –C=O amide is clear in OA/OAm and Au OA/OAm 3/1, 1/1, and 1/3 but not obvious in pure OA and Au OA/OAm 1/0, the results indicate that there is definitely interaction between OA and OAm to form OA-OAm complex,

amide, or carboxylate and amine cation. It is suspected that combination of OA and OAm at 1/1 v/v ratio can allow the most anion-cation formation and the densely and sufficiently bidentate capping of particle surface. The FT-IR result, therefore, is consistent with the observed colloidal stability and the change in particle size when moving from OA rich or OAm rich liquids to OA/OAm 1/1. This can be the second reason, aside from the highest viscosity of the OA/OAm 1/1 liquid, for the formation of the most uniform and smallest Au nanoparticles as well as their best colloidal stability over a year of storage in Au OA/OAm 1/1 sample.

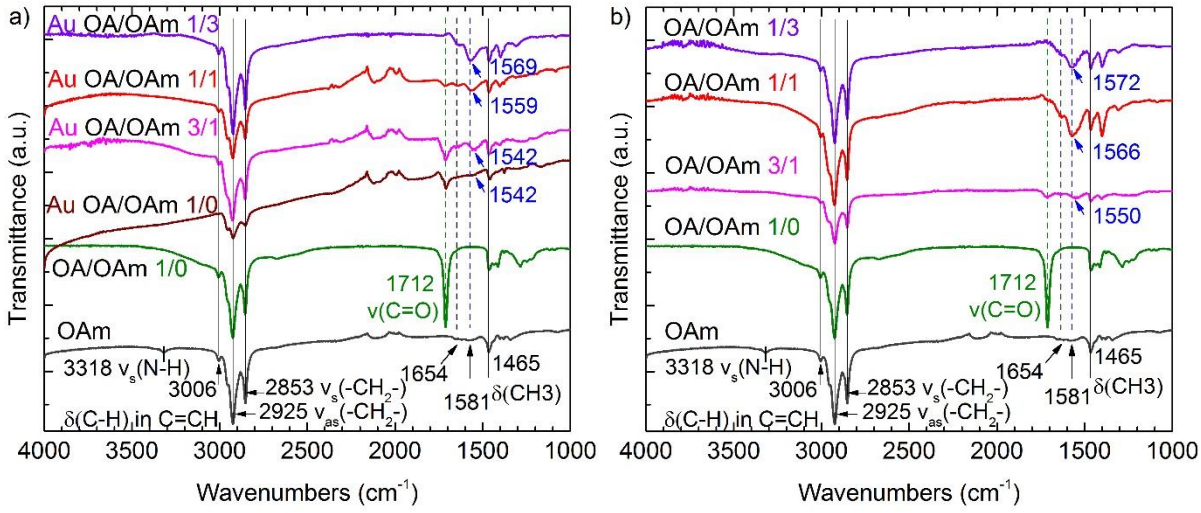

Figure 7. FT-IR spectra of (a) Au nanoparticles sputtered onto OA/OAm after 540 days of storage and (b) of pure OAm, OA/OAm 1/0, 3/1, 1/1, and 1/3 where v is the stretching mode, ν_s is symmetric stretching, ν_{as} is asymmetric stretching, and δ is the bending mode. The black solid lines mark the peaks position common in all samples. Dashed lines with green, blue, and black color are used for visual guide of the peaks position of C=O stretching in OA (1712 cm^{-1}) and -NH_2 bending in OAm (1581 cm^{-1}), and a position at 1654 cm^{-1}.

Discussion of the impact of OA/OAm on the oxidation suppression

Because Au is chemically stable, therefore, to evaluate the effect of mixing OA and OAm in chemical stabilization of metal nanoparticles, sputtering of Cu target was conducted. The results help understand oxidation stability of Cu formed in liquids with different OA/OAm volume ratio. Immediate color change to blue from the top liquid surface was observed in the dispersion of Cu OA/OAm 1/0 after the synthesis and exposure to air. UV-Vis spectra reveal the formation of Cu oleate with an absorption peak top at 680 nm for 0.5 h after the synthesis (**Figure 8**). This can occur via oxidation of Cu with air and reaction of Cu oxide with OA (scheme in **Figure 8**). The absorption peak of Cu oleate increased with exposing time and no more change was observed after one day. The mixed liquids with higher viscosity and less acidity than pure OA can be beneficial for shielding the dispersed particles from direct contact with air and particle corrosion, respectively. It was observed that mixing with OAm (OA/OAm 3/1 and 1/1) helped reduce the oxidation of Cu. UV-Vis spectra of sample Cu OA/OAm 3/1 shows that it took longer time for observing the absorption associated with Cu-oxide and/or Cu-oleate and it took 2 days for the peak to be stable. Similar phenomenon was observed for Cu OA/OAm 1/1. The peak top of Cu OA/OAm 3/1 and Cu OA/OAm 1/1 is 1/3 and 1/2 that of Cu OA/OAm 1/0, respectively. This indicates that the formation of Cu oxide and oleate was suppressed and/or occurred at a lower speed. When higher amount of OAm was used, *i.e.*, OA/OAm 1/3, UV-Vis absorption associated with oxidation and oleate formation was observed after 0.5 h and increased with time which reached the stable state after 1 day. This is similar to the phenomenon observed for Cu OA/OAm 1/0, but the peak top of Cu OA/OAm 1/3 is half that of Cu OA/OAm 1/0. Thus, the overall results of mixing OA and OAm and OA itself suggests that the deprotonation of OA by OAm to form carboxylate and amine cation for stabilizing the particle can help suppress the oxidation of Cu. However, purification of Cu for collecting the particles in powder form was challenging. As soon as solvents (hexane, acetone)

were added to Cu OA/OAm, the oxidation of Cu followed by its dissolution proceeded substantially fast, resulting in no solid material after centrifugation. This phenomenon also occurred (Figure S11) when we increased the sputter current to 100 mA for 20 min sputtering for obtaining similar mass of Cu with expecting bigger particle size, thereby, to some extent, lowering the oxidation and dissolution speed. TEM images of the as-prepared samples sputtered at 100 mA for 20 min (TEM grid was dip for ~ 40 s in hexane) show some particles left on the grid, which had similar sizes for both Cu OA/OAm1/0 and 1/1 samples. In both samples, Cu oxides were observed in SAED and HR-TEM (Figure S12). Thus, it can be concluded that OA/OAm mixture is better than pure OA in terms of slower oxidation and dissolution of Cu, however, the oxidation still occurred at high speed upon purification.

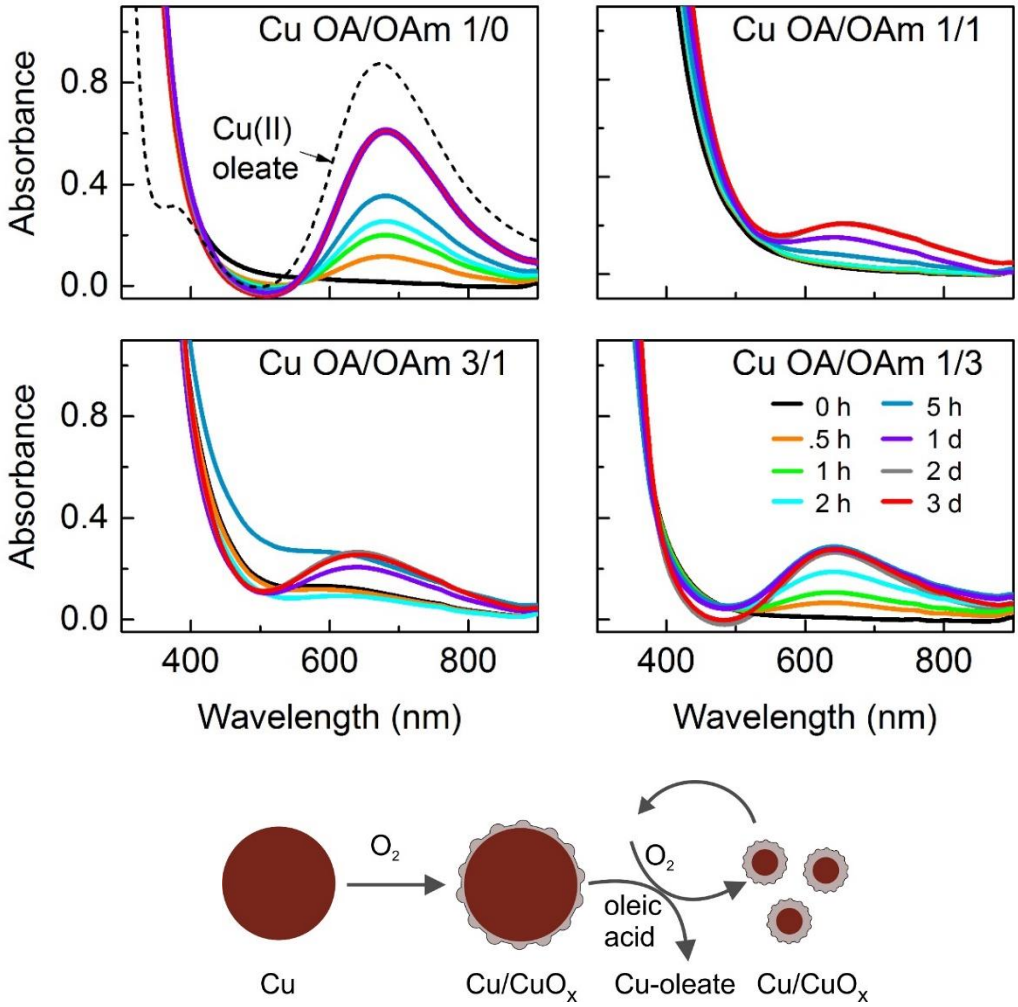

Figure 8. UV-Vis spectra of the obtained dispersions using OA/OAm with various volume ratios over time. The peak associates with the formation of Cu-oleate (in Cu OA/OAm 1/0) and/or Cu oxide (in Cu OA/OAm 3/1, 1/1, and 1/3). Black, dashed curve is the absorption spectrum of the synthesized Cu(II) oleate. The oxidation and dissolution to form oxidized compounds (copper oxides (CuO_x), and Cu-oleate) from the sputtered Cu particles in the OA containing liquids is depicted in the scheme at the bottom of the figure.

Conclusions

The results in this study indicate the advantage of mixing OA and OAm to form more viscous liquid and more powerful stabilizing capability as the matrix for sputtering of metal nanoparticles. The size control and tunability (2.4-20 nm) as well as colloidal stability were demonstrated for Au nanoparticles. The best uniformity and colloidal stability over time of Au nanoparticles were achieved for OA/OAm 1/1 in which the reasons are ascribed for high viscosity and synergistic stabilization effect by oleate and amine cations. The mixed liquid is efficient dispersing medium over a year of storage. In addition, by mixing OA and OAm, oxidation of metal nanoparticles could be suppressed compared with using only OA.

Associated Content

Supporting Information. Photograph of the synthesized samples, TEM images, size distributions, and UV-Vis spectra of Au nanoparticles stored in OA/OAm for 7 to 540 days after sputtering. HR-TEM images of big and small Au nanoparticles. Photograph, TEM, HR-TEM, and SAED of sputtered Cu particles. The following file (PDF) is available free of charge.

Author Information

Corresponding Author:

*Email: mai_nt@eng.hokudai.ac.jp, tetsu@eng.hokudai.ac.jp

Acknowledgements

This work is partially supported by Hokkaido University. We thank Mr. T. Tanioka, Mr. R. Oota, and Ms. R. Ishikawa (Hokkaido University) for their technical assistance in TEM observations, Mr. S. Kimura (Hokkaido University) for fruitful discussions. KW and VA thank CEED, Hokkaido University for financial support for their stays in Sapporo. MTN

acknowledge partial financial support by Grant-in-Aid for Scientific Research for Young Researcher (B) from JSPS (17K14072), Young Research Acceleration Project of Hokkaido University, Grant for Basic Science Research Projects from the Sumitomo foundation, and the Kurata Grant awarded by the Hitachi Global Foundation. TY thanks partial financial support by Grant-in-Aid for Scientific Research (B) (18H01820) and Grant-in-Aid for Scientific Research on Innovative Areas (Research in a proposed research area) (19H05162) from JSPS.

Conflict of Interest

There is no conflict of interest to declare.

References

1. Wagener, M.; Günther, B. Sputtering on Liquids - a Versatile Process for the Production of Magnetic Suspensions? *J. Magn. Magn. Mater.*, **1999**, *201*, 41-44.
2. Torimoto, T.; Okazaki, K.; Kiyama, T.; Hirahara, K.; Tanaka, N.; Kuwabata, S. Sputter Deposition onto Ionic Liquids: Simple and Clean Synthesis of Highly Dispersed Ultrafine Metal Nanoparticles. *Appl. Phys. Lett.*, **2006**, *89*, 243117−1−3.
3. Okazaki, K.; Kiyama, T.; Hirahara, K.; Tanaka, N.; Kuwabata, S.; Torimoto, T. Single-step synthesis of gold-silver alloy nanoparticles in ionic liquids by a sputter deposition technique. *Chem. Commun.*, **2008**, 691–693.
4. Shishino, Y.; Yonezawa, T.; Kawai, K.; Nishihara, H. Molten Matrix Sputtering Synthesis of Water-soluble Luminescent Au Nanoparticles with a Large Stokes Shift. *Chem. Commun.*, 2010, **46**, 7211-7213.
5. Wender, H.; de Oliveira, L. F.; Feil, A. F.; Lissner, E.; Migowski, P.; Meneghetti, M. R.; Teixeira, S. R.; Dupont, J. Synthesis of Gold Nanoparticles in a Biocompatible Fluid from Sputtering Deposition onto Castor Oil. *Chem. Commun.*, **2010**, *46*, 7019-7021.

6. Hatakeyama, Y.; Morita , T.; Takahashi, S.; Onishi, K.; Nishikawa, K. Synthesis of Gold Nanoparticles in Liquid Polyethylene Glycol by Sputter Deposition and Temperature Effects on their Size and Shape. *J. Phys. Chem. C*, **2011**, *115* , 3279- 3285.
7. Wender, H.; Goncalves, R. V.; Feil, A. F.; Migowski, P.; Poletto, F. S.; Pohlmann, A. R.; Dupont, J.; Teixeira, S. R. Sputtering onto Liquids: From Thin Films to Nanoparticles. *J. Phys. Chem. C*, **2011**, *115*, 16362-16367.
8. Hamm, S. C.; Shankaran, R.; Korampally, V.; Bok, S.; Praharaj, S.; Baker, G. A.; Robertson, J. D.; Lee, B. D.; Sengupta, S.; Gangopadhyay, K.; Gangopadhyay, S. Sputter-deposition of silver nanoparticles into ionic liquid as a sacrificial reservoir in antimicrobial organosilicate nanocomposite coatings. *ACS. Appl. Mater. Interfaces,* **2012**, *4*, 178–184.
9. Staszek, M.; Siegel, J.; Kolárová, K.; Rimpelová, S.; Švorcík, V. Formation and antibacterial action of Pt and Pd nanoparticles sputtered into liquid. *Micro Nano Lett.*, **2014**, *9*, 778-781.
10. Yoshii, K.; Yamaji, K.; Tsuda, T.; Matsumoto, H.; Sato, T.; Izumi, R.; Torimoto, T.; Kuwabata, S. Highly durable Pt nanoparticle-supported carbon catalyst for the oxygen reduction reaction tailored by using an ionic liquid thin layer. *J. Mater. Chem. A*, **2016**, *4*, 12152-12157.
11. Wender, H.; Migowski, P.; Feil, A. F.; Teixeira, S. R.; Dupont, J. Sputtering Deposition of Nanoparticles onto Liquid Substrates: Recent Advances and Future Trends. *Coord. Chem. Rev.*, **2013**, *257*, 2468-2483.
12. Nguyen, M. T.; Yonezawa, T. Sputtering onto a liquid: interesting physical preparation method for multi-metallic nanoparticles. *Sci. Technol. Adv. Mater.*, **2018**, *19*, 465-496.
13. Ishida, Y.; Corpuz, R. D.; Yonezawa, T. Matrix Sputtering Method: A Novel Physical Approach for Photoluminescent Noble Metal Nanoclusters. *Acc. Chem. Res.*, **2017**, *50*, 2986-2995.
14. Porta, M.; Nguyen, M. T.; Yonezawa, T.; Tokunaga, T.; Ishida, Y.; Tsukamoto, H.; Shishino, Y.; Hatakeyama, Y. Titanium Oxide Nanoparticle Dispersions in a Liquid Monomer and Solid Polymer Resin Prepared by Sputtering. *New J. Chem.*, **2016**, *40*, 9337-9343.

15. Porta, M.; Nguyen, M. T.; Tokunaga, T.; Ishida, Y.; Liu, W.-R.; Yonezawa, T. Matrix Sputtering into Liquid Mercaptan: From Blue-Emitting Copper Nanoclusters to Red-Emitting Copper Sulfide Nanoclusters. *Langmuir*, **2016**, *32*, 12159-12165.
16. Suzuki, S.; Suzuki, T.; Tomita, Y.; Hirano, M.; Okazaki, K.; Kuwabata, S.; Torimoto, T. Compositional control of AuPt nanoparticles synthesized in ionic liquids by the sputter deposition technique. *CrystEngComm*, **2012**, *14*, 4922-4926.
17. Hirano, M.; Enokida, K.; Okazaki, K.; Kuwabata, S.; Yoshida, H.; Torimoto, T. Composition-dependent electrocatalytic activity of AuPd alloy nanoparticles prepared *via* simultaneous sputter deposition into an ionic liquid. *Phys. Chem. Chem. Phys.*, **2013**, *15*, 7286-7294.
18. König, D.; Richter, K.; Siegel, A.; Mudring, A. V.; Ludwig, A. High-throughput fabrication of Au-Cu nanoparticle libraries by a combinatorial sputtering in ionic liquids. *Adv Funct Mater.*, **2014**, *24*, 2049–2056.
19. Suzuki, S.; Tomita, Y.; Kuwabata, S.; Torimoto, T. Synthesis of alloy AuCu nanoparticles with the $L1_0$ structure in an ionic liquid using sputter deposition. *Dalton Trans.*, **2015**, *44*, 4186-4194.
20. Liu, C. H.; Liu, R. H.; Sun, Q. J.; Chang, J. B.; Gao, X.; Liu, Y.; Lee, S. T.; Kang, Z. H.; Wang. S. D. Controlled synthesis and synergistic effects of graphene-supported PdAu bimetallic nanoparticles with tunable catalytic properties. *Nanoscale*, **2015**, *7*, 6356-6362.
21. Torimoto, T.; Ohta, Y.; Enokida, K.; Sugioka, D.; Kameyama, T.; Yamamoto, T.; Shibayama, T.; Yoshii, K.; Tsuda, T.; Kuwabata, S. Ultrathin oxide shell coating of metal nanoparticlesusing ionic liquid/metal sputtering. *J. Mater. Chem. A*, **2015**, *3*, 6177-6186
22. Nguyen, M. T.; Yonezawa, T.; Wang, Y.; Tokunaga, T. Double Target Sputtering into Liquid: A New Approach for Preparation of Ag-Au Alloy Nanoparticles. *Mater. Lett.*, **2016**, *171*, 75-78.
23. Nguyen, M. T.; Zhang, H.; Deng, L.; Tokunaga, T.; Yonezawa, T. Au/Cu Bimetallic Nanoparticles via Double Target Sputtering onto a Liquid Polymer. *Langmuir*, **2017**, *33*, 12389-12397.
24. Löffler, T.; Meyer, H.; Savan, A.; Wilde, P.; Manjón, A. G.; Chen, Y.-T.; Ventosa, E.; Scheu, C.; Ludwig, A.; Schuhmann, W. Discovery of a Multinary Noble Metal–Free Oxygen Reduction Catalyst. *Adv. Energy Mater*., **2018**, *8*, 1802269 (7 pages).

25. Iimori, T.; Hatakeyama, Y.; Nishikawa, K.; Kato, M.; Ohta, N. Visible Photoluminescence of Gold Nanoparticles Prepared by Sputter Deposition Technique in a Room-Temperature Ionic Liquid. *Chem. Phys. Lett.*, **2013**, *586*, 100-103.
26. Sumi, T.; Motono, S.; Ishida, Y.; Shirahata, N.; Yonezawa, T. Formation and Optical Properties of Fluorescent Gold Nanoparticles Obtained by Matrix Sputtering Method with Volatile Mercaptan Molecules in the Vacuum Chamber and Consideration of Their Structures. *Langmuir*, **2015**, *31*, 4323-4329.
27. Hatakeyama, Y.; Takahashi, S.; Nishikawa, K. Can Temperature Control the Size of Au Nanoparticles Prepared in Ionic Liquids by the Sputter Deposition Technique? *J. Phys. Chem. C*, **2010**, *114*, 11098-11102.
28. Wender, H.; de Oliveira, L. F.; Migowski, P.; Feil, A. F.; Lissner, E.; Prechtl, M. H. G.; Teixeira, S. R.; Dupont, J. Ionic Liquid Surface Composition Controls the Size of Gold Nanoparticles Prepared by Sputtering Deposition. *J. Phys. Chem. C*, **2010**, *114*, 11764-11768
29. Vanecht, E.; Binnemans, K.; Seo, J. W.; Stappers, L.; Fransaer, J. Growth of sputter-deposited gold nanoparticles in ionic liquids. *Phys. Chem. Chem. Phys.*, **2011**, *13*, 13565-13571.
30. Sugioka, D.; Kameyama, T.; Kuwabata, S.; Torimoto, T. Single-step preparation of two-dimensionally organized gold particles via ionic liquid/metal sputter deposition. *Phys. Chem. Chem. Phys.*, **2015**, *17*, 13150-13159.
31. Hatakeyama, Y.; Judai, K.; Onishi, K.; Takahashi, S.; Kimura, S.; Nishikawa, K. Anion and cation effects on the size control of Au nanoparticles prepared by sputter deposition in imidazolium-based ionic liquids. *Phys. Chem. Chem. Phys.*, **2016**, *18*, 2339-2349.
32. Hatakeyama, Y.; Kimura, S.; Kameyama, K.; Agawa, Y.; Tanaka, H.; Judai, K.; Torimoto, T.; Nishikawa, K. Temperature-independent formation of Au nanoparticles in ionic liquids by arc plasma deposition. *Chem. Phys. Lett.*, **2016**, *658*, 188-191.
33. De Luna, M. M.; Gupta, M. Effects of surface tension and viscosity on gold and silver sputtered onto liquid substrates. *Appl. Phys. Lett.*, **2018**, *112*, 201605.

34. Deng, L.; Nguyen, M. T.; Mei, S.; Tokunaga, T.; Kudo, M.; Matsumura, S.; Yonezawa, T. Preparation and Growth Mechanism of Pt/Cu Alloy Nanoparticles by Sputter Deposition onto a Liquid Polymer. *Langmuir*, **2019**, *35*, 8418-8427.
35. Ishida, Y.; Udagawa, S.; Yonezawa, T. Growth of sputtered silver nanoparticles on a liquid mercaptan matrix with controlled viscosity and sputter rate. *Colloids Surf. A*, **2016**, *498*, 106-111.
36. Porta, M.; Nguyen, M. T.; Ishida, Y.; Yonezawa, T. Highly Stable and Blue-emitting Copper Nanocluster Dispersion Prepared by Magnetron Sputtering over Liquid Polymer Matrix. *RSC Adv.*, **2016**, *6*, 105030-105034.
37. Ishida, Y.; Nakabayashi, R.; Matsubara, M.; Yonezawa, T. Silver sputtering into a liquid matrix containing mercaptans: the systematic size control of silver nanoparticles in single nanometer-orders. *New J. Chem.*, **2015**, *39*, 4227-4230.
38. Corpuz, R. D.; Ishida, Y.; Nguyen, M. T.; Yonezawa, T. Synthesis of positively charged photoluminescent bimetallic Au-Ag nanoclusters by double target sputtering method on a biocompatible polymer matrix. *Langmuir*, **2017**, *33*, 9144-9150.
39. Deng, L.; Nguyen, M. T.; Shi, J.; Chau, Y.-t. R.; Tokunaga, T.; Kudo, M.; Matsumura, S.; Hashimoto, N.; Yonezawa, T. Highly Correlated Size and Composition of Pt/Au Alloy Nanoparticles via Magnetron Sputtering onto Liquid. *Langmuir*, **2020**, *36*, 3004-3015.
40. Fujita, A.; Matsumoto, Y.; Takeuchi, M.; Ryuto, H.; Takaoka, G. H. Growth behavior of gold nanoparticles synthesized in unsaturated fatty acids by vacuum evaporation methods. *Phys. Chem. Chem. Phys.*, **2016**, *18*, 5464-5470.
41. Gawande, M. B.; Goswami, A.; Felpin, F.-X.; Asefa, T.; Huang, X.; Silva, R.; Zou, X.; Zboril, R.; Varma, R. S. Cu and Cu-Based Nanoparticles: Synthesis and Applications in Catalysis. *Chem. Rev.*, **2016**, *116*, 3722-3811.
42. Nakagawa, K.; Narushima, T.; Udagawa, S.; Yonezawa, T. Preparation of Copper Nanoparticles in Liquid by Matrix Sputtering Process. *J. Phys.: Conf. Ser.*, **2013**, *417*, 012038.
43. Chau, Y.-T. R.; Deng, L.; Nguyen, M. T.; Yonezawa, T. Monitor the Growth and Oxidation of Cu-nanoparticles in PEG after Sputtering. *Mater. Res. Soc. Adv.*, **2019**, *4*, 305-309.

44. Harris, R. A.; Shumbula, P. M.; van der Walt, H. Analysis of the Interaction of Surfactants Oleic Acid and Oleylamine with Iron Oxide Nanoparticles through Molecular Mechanics Modeling. *Langmuir*, **2015**, *31*, 3934-3943.

45. Park, J.; An, K.; Hwang, Y.; Park, J.-G.; Noh, H.-J.; Kim, J.-Y.; Park, J.-H.; Hwang, N.-M.; Hyeon, T. Ultra-large-scale Syntheses of Monodisperse Nanocrystals. *Nature Mater*. **2004**, *3*, 891-895.

46. Bagaria, H. G.; Ada, E. T.; Shamsuzzoha, M.; Nikles, D. E.; Johnson, D. T. Understanding Mercapto Ligand Exchange on the Surface of FePt Nanoparticles. *Langmuir*, **2006**, *22*, 7732-7737.

47. Bu, W.; Chen, Z.; Chen, F.; Shi, J. Oleic Acid/Oleylamine Cooperative-Controlled Crystallization Mechanism for Monodisperse Tetragonal Bipyramid $NaLa(MoO_4)_2$ Nanocrystals. *J. Phys. Chem. C* **2009**, *113*, 12176–12185.

48. Liu, J.; Zhang, W.; Zhang, H.; Yang, Z.; Li, T.; Wang, B.; Huo, X.; Wang, R.; Chen, H. A multifunctional nanoprobe based on Au–Fe_3O_4 nanoparticles for multimodal and ultrasensitive detection of cancer cells. *Chem. Commun.*, **2013**, *49*, 4938-4940.

49. Lu, X.; Tuan, H.-Y.; Korgel, B. A.; Xia, Y. Facile Synthesis of Gold Nanoparticles with Narrow Size Distribution by Using AuCl or AuBr as the Precursor. *Chemistry*, **2008**, *14*, 1584–1591.

Figure for the Table of Contents use only

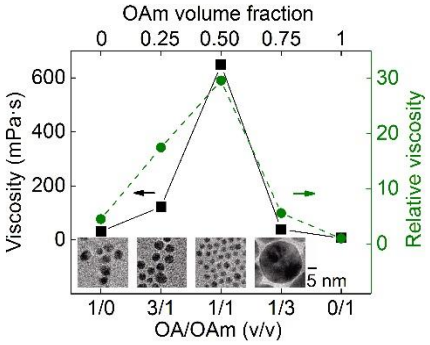

Synopsis: Viscosity and interaction of oleic acid and oleylamine matrix help control particle size and stability of the sputtered metal nanoparticles.